Eur. J. Mineral.
2015, **27**, 581–588
Published online 30 April 2015

New zinc and potassium chlorides from fumaroles of the Tolbachik volcano, Kamchatka, Russia: mineral data and crystal chemistry. II. Flinteite, K_2ZnCl_4

IGOR V. PEKOV[1,*], NATALIA V. ZUBKOVA[1], VASILIY O. YAPASKURT[1], SERGEY N. BRITVIN[2,3], MARINA F. VIGASINA[1], EVGENY G. SIDOROV[4] and DMITRY YU. PUSHCHAROVSKY[1]

[1] Faculty of Geology, Moscow State University, Vorobievy Gory, 119991 Moscow, Russia
*Corresponding author, e-mail: igorpekov@mail.ru
[2] Department of Crystallography, St Petersburg State University, Universitetskaya Nab. 7/9, 199034 St Petersburg, Russia
[3] Nanomaterials Research Center, Kola Science Center of Russian Academy of Sciences, Fersman Str. 18, 184209 Apatity, Russia
[4] Institute of Volcanology and Seismology, Far Eastern Branch of Russian Academy of Sciences, Piip Boulevard 9, 683006 Petropavlovsk-Kamchatsky, Russia

Abstract: The new mineral flinteite, ideally K_2ZnCl_4, was discovered in active fumaroles at two scoria cones of the Northern Breakthrough of the Great Tolbachik Fissure Eruption, Tolbachik volcano, Kamchatka, Russia. In the Northern fumarole field at the First scoria cone (locality of the holotype), flinteite is a common mineral associated with halite, sellaite, fluorite, saltonseaite, chubarovite and hollandite. In the Arsenatnaya fumarole at the Second scoria cone, flinteite occurs with langbeinite, aphthitalite, fluoborite, sylvite, halite, tenorite, hematite, zincite, chubarovite, krasheninnikovite, vanthoffite, *etc*. In the Glavnaya Tenoritovaya fumarole (Second scoria cone), flinteite is associated with mellizinkalite, belloite, avdoninite, eriochalcite, sylvite, halite, mitscherlichite, sanguite, chrysothallite, romanorlovite, gypsum, chlorothionite, kainite, *etc*. Flinteite typically forms prismatic crystals up to $0.2 \times 0.3 \times 1.2$ mm, their groups, granular aggregates or crusts up to $0.5 \times 5 \times 5$ mm. The mineral is light green, light yellow to bright greenish-yellow or colourless. It is transparent, with vitreous lustre. Flinteite is brittle, one direction of distinct cleavage was observed. The Mohs hardness is *ca.* 2. $D_{calc} = 2.49$ g cm^{-3}. Flinteite is optically biaxial (+), $\alpha = 1.573(1)$, $\beta = 1.574(1)$, $\gamma = 1.576(1)$, $2V_{meas} = 40(25)^\circ$. The chemical composition of the holotype (wt%, electron-microprobe data) is: K 24.97, Tl 5.82, Co 0.07, Zn 22.23, Cl 46.95, total 100.04. The empirical formula calculated based on the sum of all atoms = 7 *pfu* is: $(K_{1.91}Tl_{0.09})_{\Sigma 2.00}Zn_{1.04}Cl_{3.96}$. Some samples show the following substitutions for K (wt%): up to 27.7 Tl, 0.6–2.4 Rb, 0.5–2.2 Cs. Flinteite is orthorhombic, $Pna2_1$, $a = 26.8090(10)$, $b = 12.4085(6)$, $c = 7.2512(3)$ Å, $V = 2412.18(18)$ Å^3 and $Z = 12$. The strongest reflections of the powder X-ray diffraction pattern [*d*,Å(*I*)(*hkl*)] are: 6.23(27)(011, 020), 5.123(88)(311, 320), 3.629(98)(611, 002), 3.599(100)(031), 3.133(35)(022), 3.039(26)(630), 2.897(35)(910) and 2.688(46)(911, 920). The crystal structure, solved from single-crystal X-ray diffraction data ($R = 0.0686$), contains three Zn sites centring isolated $ZnCl_4$ tetrahedra and six independent K sites. Flinteite is the natural analogue of a well-known synthetic room-temperature modification of K_2ZnCl_4, a ferroelectric material. The mineral is named in honour of the Russian crystallographer Evgeniy E. Flint (1887–1975).

Key-words: flinteite; new mineral; potassium zinc chloride; thallium in potassium mineral; crystal structure; fumarole; Tolbachik volcano; Kamchatka.

Introduction

This paper is the second one in a series of coupled articles on mineralogy and crystal chemistry of new zinc and potassium chlorides from active fumaroles located at the scoria cones of the Northern Breakthrough of the Great Tolbachik Fissure Eruption of 1975–76 (NB GTFE), Tolbachik volcano, Kamchatka Peninsula, Far-Eastern Region, Russia. General data on zinc mineralization in these fumaroles are reported in the first paper of the series devoted to mellizinkalite, $K_3Zn_2Cl_7$ (Pekov *et al.,* 2015a).

In the present article we describe a new mineral species, flinteite[1] (Cyrillic: флинтеит), named in honour of the Russian crystallographer Evgeniy Evgenievich Flint (1887–1975), Professor of Crystallography in Moscow State University (1925–1930), Professor of Mineralogy and Crystallography in Moscow Geological Prospecting

[1] The mineral was named flinteite (constructed from: Flint, E.) but not ''flintite'' because the latter could give the incorrect impression that it is a rock consisting of flint; moreover, ''flintite'' is phonetically similar to the mineral name flinkite.

DOI: 10.1127/ejm/2015/0027-2459
0935-1221/15/0027-2459 $ 3.60

Institute (1930–1962) and Senior Researcher in Institute of Crystallography of the USSR Academy of Sciences (1938–1962). He was a specialist in goniometry (in particular, a constructor of four novel goniometer models) and X-ray crystallography. Prof. Flint also studied the piezoelectric properties of quartz and compiled a catalogue of pyroelectric and piezoelectric crystals including almost 1000 species.

Both the new mineral and its name have been approved by the IMA Commission on New Minerals, Nomenclature and Classification (IMA2014–009). The type specimen of flinteite is deposited in the systematic collection of the Fersman Mineralogical Museum of the Russian Academy of Sciences, Moscow, with the catalogue number 94374.

Fig. 1. Prismatic crystals of flinteite with halite on volcanic scoria. The holotype specimen from Northern fumarole field, First scoria cone. Field of view: 2.4 mm. Photograph: I.V. Pekov & A.V. Kasatkin. (online version in colour)

Occurrence and general appearance

The specimen that became the holotype of flinteite was found by us in July 2013 in one of active fumaroles belonging to the Northern fumarole field located on the northern slope of the crater of the First scoria cone of the NB GTFE. In July 2014 we ascertained that the new mineral is widespread in fumaroles of this field and also found flinteite in small amounts in two fumaroles, Arsenatnaya and Glavnaya Tenoritovaya (''Major Tenorite'') at the apical part of the Second scoria cone of the NB GTFE.

The two scoria cones are neighbouring monogenetic volcanoes formed in 1975, each about 300 m high and approximately 0.1 km^3 in volume. They are situated 18 km SSW of the active volcano Ploskiy Tolbachik (Fedotov & Markhinin, 1983). These scoria cones demonstrate strong fumarolic activity to the present day. Our measurements on gas vents, performed using chromel-alumel thermocouple during the 2012–2014 fieldworks, showed temperatures up to 430°C at the Second scoria cone and up to 300°C at the First scoria cone.

The most mineralized areas in fumaroles of the Northern field of the First scoria cone occur at depths of 0.1–0.3 m below the surface. The major exhalation minerals, forming incrustations on basalt scoria altered by volcanic gas, are sellaite, fluorite, halite and anhydrite. Cotunnite, sofiite and, sporadically, flinteite are present in subordinate amounts. Rare sublimate minerals are chubarovite $KZn_2(BO_3)Cl_2$ (IMA2014–018), anglesite, challacolloite, zincomenite $ZnSeO_3$ (IMA2014–014), saltonseaite, hollandite, hematite, jakobssonite, leonardsenite and olsacherite. Thus, the fumarolic mineralization here is represented mainly by chlorides, fluorides, and sulphates with subordinate selenites, oxides, and borates and the major species-defining cations of minerals are Ca, Mg, Na, K, Zn, Pb, and Mn. Flinteite occurs in open pockets and cracks at the depths 0.1–0.2 m below day surface. The temperatures measured inside these pockets immediately after their uncovering (July 2014) were 270–290°C. The new mineral overgrows basalt scoria (Figs 1 and 2a) or massive white or grey crusts mainly consisting of sellaite and fluorite. It is typically closely associated with halite, saltonseaite $K_3NaMnCl_6$, chubarovite and hollandite.

Mineral assemblages with flinteite in the fumaroles of the Second scoria cone significantly differ from the above reported.

In the Arsenatnaya fumarole (for its description see Pekov *et al.*, 2014a), the new mineral was found in two associations formed in open pockets. In the northern part of the fumarole flinteite occurs with krasheninnikovite, langbeinite, aphthitalite, arcanite, sylvite, halite, tenorite, zincite, fluoborite, chubarovite, wulffite $K_3NaCu_4O_2(SO_4)_4$ (IMA2013–035), johillerite, and urusovite. All these minerals overgrow crusts of earlier sublimate minerals represented by orthoclase, fluorophlogopite, hematite, and pseudobrookite. In the southern part of Arsenatnaya, flinteite is associated with halite, langbeinite, aphthitalite, vanthoffite, fluoborite and subordinate calciolangbeinite, sylvite, chubarovite, zincite, svabite, and hematite. In both cases flinteite was observed on sulphate incrustations. The temperatures measured inside different pockets with these mineral associations varied from 300 to 360°C.

In the Glavnaya Tenoritovaya fumarole, flinteite was found in the sulphate–chloride zone (Pekov *et al.*, 2015b). Unlike all abovementioned high-temperature assemblages consisting of only anhydrous minerals, H-bearing minerals are abundant here which is caused by relatively low temperature: 110°C, from our measurements. The major minerals are belloite, avdoninite, eriochalcite, sylvite, halite, carnallite, sanguite $KCuCl_3$ (IMA2013–002), gypsum, chlorothionite and kainite, whereas sellaite, mitscherlichite, chrysothallite $K_6Cu_6Tl^{3+}Cl_{17}(OH)_4 \cdot H_2O$ (Pekov *et al.*, 2015b), romanorlovite $K_8Cu_6Cl_{17}(OH)_3$ (IMA2014–011), mellizinkalite, flinteite and an incompletely studied K-Pb-Cu hydroxychloride are subordinate. Flinteite was found in

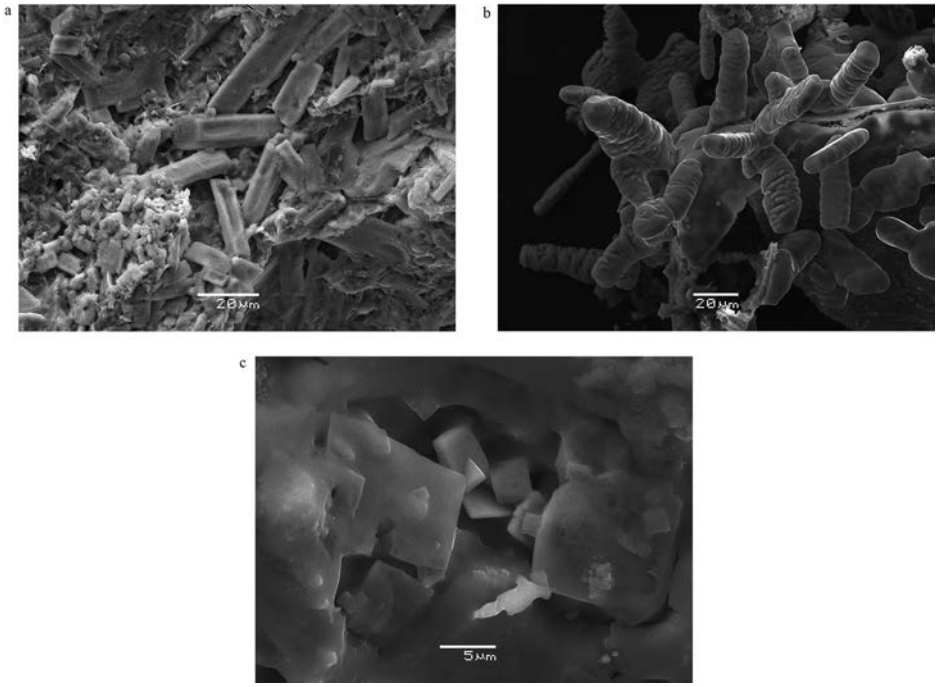

Fig. 2. Morphology of flinteite from Northern fumarole field, First scoria cone: (a) prismatic crystals on volcanic scoria; (b) cluster of crude, complicated individuals; (c) tabular crystals of a Tl-rich variety. SEM (SE) images.

small cavities of the sulphate–chloride aggregates in intimate intergrowths with mellizinkalite, $K_3Zn_2Cl_7$.

Flinteite typically occurs as prismatic to long-prismatic crystals up to $0.2 \times 0.3 \times 1.2$ mm in size, their groups (Figs 1 and 2a and b), irregularly shaped grains and granular or near-parallel, columnar aggregates or crusts up to 5×5 mm in area and up to 0.5 mm thick. Equant or tabular crystals (Fig. 2c) are less common. Coarse individuals, with uneven surface and roundish contour (Fig. 2b) are usual. Signs of skeletal growth were observed on some crystals (Fig. 2a).

Physical properties and optical characteristics

Flinteite is typically light green (sometimes apple green or light bluish-green), light yellow to bright greenish-yellow or colourless. Its streak is white. The mineral is transparent, with vitreous lustre. Flinteite is brittle. The Mohs hardness is *ca.* 2. One direction of distinct cleavage was observed under the microscope. The fracture is uneven. Density was not measured because the largest particles of the mineral contain inclusions of fragments of porous volcanic scoria. The density calculated for the holotype sample using the empirical formula is 2.49 g cm^{-3}.

Flinteite is optically biaxial (+), $\alpha = 1.573(1)$, $\beta = 1.574(1)$, $\gamma = 1.576(1)$ (589 nm), $2V_{meas} = 40(25)^\circ$ and $2V_{calc} = 71^\circ$. The low precision in the measurement of $2V$ and the discrepancy between $2V_{meas}$ and $2V_{calc}$ are caused by the low birefringence of the mineral. No dispersion of optical axes was observed. Under the microscope flinteite is colourless and non-pleochroic.

Raman spectroscopy

The Raman spectrum of flinteite (Fig. 3) was obtained from a randomly oriented crystal using an EnSpectr R532 instrument (Dept. of Mineralogy, Moscow State University) with a green laser (532 nm) at room temperature. The power of the laser beam on the sample was about 13 mW. The spectrum was processed using the EnSpectr expert mode program in the range from 100 to 4000 cm^{-1} with the use of a holographic diffraction grating with 1800 lines cm^{-1} and spectral resolution of 5–8 cm^{-1}. The diameter of the focal spot on the sample was about 15 μm.

All absorption bands in the Raman spectrum of flinteite have maxima below 300 cm^{-1}. The intense, narrow band at 294 cm^{-1} corresponds to Zn–Cl stretching vibrations, and

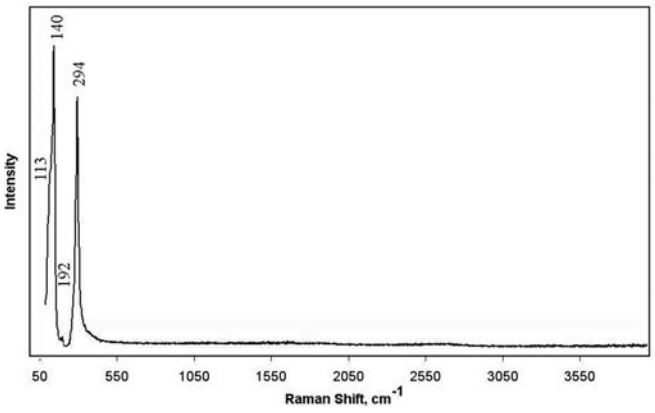

Fig. 3. The Raman spectrum of flinteite.

bands with frequencies below 200 cm^{-1} (at 192, 140 and 113 cm^{-1}) correspond to lattice modes, Zn–Cl bending and K–Cl stretching vibrations. The bands are assigned according to the data reported for $ZnCl_2$ and K-Zn chlorides by Moyer *et al.* (1966). An absence of absorption bands in the region higher than 600 cm^{-1} indicates the absence of groups with O–H, C–H, C–O, N–H, N–O, B–O, Be–O and Li–O bonds in the mineral.

Chemical data

Chemical data for flinteite were obtained using a Jeol JSM-6480LV scanning electron microscope equipped with an INCA-Wave 500 wavelength-dispersive spectrometer (Laboratory of local methods of matter investigation, Faculty of Geology, Moscow State University). The wavelength-dispersive (WDS) mode was used, with an acceleration voltage of 20 kV, a beam current of 20 nA, and a 5 μm beam diameter. The following standards were used: microcline (K), $Rb_2Nb_4O_{11}$ (Rb), $Cs_2Nb_4O_{11}$ (Cs), $TlAsS_2$ (Tl), Co (Co), $CuFeS_2$ (Cu), ZnSe (Zn), and NaCl (Cl).

The electron-microprobe data for chemically different varieties of flinteite are given in Table 1. The empirical formula of the holotype sample calculated based on the sum of all atoms = 7 *pfu* is $(K_{1.91}Tl_{0.09})_{\Sigma 2.00}Zn_{1.04}Cl_{3.96}$.

Significant substitution of potassium by larger monovalent cations is common for flinteite. In fumaroles of the First scoria cone, thallium is a typical admixture in this mineral. Its concentration varies in a wide range, from 0.3 to 27.7 wt% (0.00–0.51 *apfu*) and demonstrates clear negative correlation with K content (##1–5 in Table 1). The crystal structure data (see below) confirm the Tl^+–K substitution in flinteite. The Tl-richest varieties of the mineral typically form tabular crystals (Fig. 2c). Samples from fumaroles of the Second scoria cone are Tl-poor but contain up to 2.4 wt% Rb (=0.08 *apfu*) and up to 2.2 wt% Cs (=0.05 *apfu*): ##6–8 in Table 1. Contents of admixed elements substituting zinc are minor: no more than 0.04 *apfu* Cu + Co (#5 in Table 1).

Flinteite dissolves very easily in H_2O at room temperature and is unstable in a humid atmosphere. Cryobostryxite $KZnCl_3 \cdot 2H_2O$ (IMA2014–058) is the most common product of the low-temperature (supergene) alteration of flinteite in the upper zone of the deposits of fumaroles belonging to the Northern field of the First scoria cone.

X-ray crystallography and crystal structure

The X-ray powder diffraction study of flinteite was carried out on a Rigaku R-AXIS Rapid II single-crystal diffractometer equipped with cylindrical image-plate detector using Debye-Scherrer geometry (d = 127.4 mm; Co$K\alpha$ radiation). X-ray powder diffraction data are given in Table 2. The unit-cell parameters refined from the powder data are: $a = 26.827(6)$, $b = 12.405(3)$, $c = 7.252(1)$ Å and $V = 2413(1)$ Å^3.

Table 1. Chemical composition of flinteite.

No.	1	2	3	4	5	6	7	8	9
Sample	#4001: holotype	#4386	#4196	#4193	#4001a	#3969a	#4323	#4306	
wt %									
K	24.97 (23.53–25.94)	28.34	26.74	20.25	16.34	26.61	25.09	24.48	27.40
Rb						0.64	2.33	2.44	
Cs							0.49	2.16	
Tl	5.82 (5.27–6.11)	0.31	3.05	15.33	27.74			0.53	
Co	0.07 (0.00–0.29)				0.52				
Cu		0.32			0.24	0.20	0.08		
Zn	22.23 (21.48–23.00)	22.51	22.74	20.94	16.70	22.69	23.29	22.72	22.91
Cl	46.95 (45.76–47.60)	49.71	48.12	43.21	37.20	49.31	47.80	48.57	49.69
Total	100.04	101.19	100.65	99.73	98.74	99.45	99.08	100.90	100.00
Formula calculated based on the sum of all atoms = 7 *pfu*									
K	1.91	2.05	1.99	1.70	1.56	1.96	1.89	1.83	2
Rb						0.02	0.08	0.08	
Cs							0.01	0.05	
Tl	0.09	0.00	0.04	0.25	0.51			0.01	
Σ*A*	***2.00***	***2.05***	***2.03***	***1.95***	***2.07***	***1.98***	***1.98***	***1.97***	***2***
Co	0.00				0.03				
Cu		0.01			0.01	0.01	0.00		
Zn	1.04	0.97	1.01	1.05	0.96	1.00	1.05	1.02	1
Σ*M*	***1.04***	***0.98***	***1.01***	***1.05***	***1.00***	***1.01***	***1.05***	***1.02***	***1***
Cl	3.96	3.97	3.96	4.00	3.93	4.01	3.97	4.01	4

1–5 – Northern fumarole field, First scoria cone (1 – average value from 4 spot analyses for the holotype sample, ranges are in parentheses); 6–8 – Second scoria cone (6 – Glavnaya Tenoritovaya fumarole; 7 – Arsenatnaya fumarole, northern part; 8 – Arsenatnaya fumarole, southern part); 9 – calculated values for the idealized formula K_2ZnCl_4. $\Sigma A = K + Rb + Cs + Tl$, $\Sigma M = Zn + Cu + Co$. Empty cell means that the concentration of element is below its detection limit (*bdl*). Contents of other elements with atomic numbers higher than carbon are *bdl* in all analyses.

Table 2. X-ray powder diffraction data for flinteite.

I_{obs}	d_{obs}	I_{calc}*	d_{calc}**	*h k l*
27	6.23	11, 19	6.261, 6.204	011, 020
88	5.123	50, 27	5.127, 5.096	311, 320
2	4.954	1	4.922	510
4	4.654	3	4.643	121
24	4.468	21	4.468	600
9	4.194	5, 3	4.204, 4.170	610, 321
20	3.802	11	3.804	601
98	3.629	38, 2, 54	3.637, 3.626, 3.626	611, 620, 002
100	3.599	100	3.593	031
11	3.497	5	3.500	202
25	3.468	9, 5	3.470, 3.451	231, 112
13	3.246	7	3.243	621
11	3.196	6	3.189	402
35	3.133	38	3.130	022
19	3.103	17	3.102	040
26	3.039	32	3.035	630
13	2.984	6	2.973	721
22	2.946	6, 16, 10	2.954, 2.954, 2.931	811, 322, 340
35	2.897	40	2.896	910
11	2.841	5	2.836	422
11	2.818	5	2.815	602
25	2.746	33	2.746	612
25	2.720	29	2.717	341
46	2.688	44, 31	2.690, 2.685	911, 920
9	2.610	10	2.608	332
20	2.564	30	2.564	622
8	2.519	4	2.518	921
8	2.417	8	2.417	930
5	2.396	3, 6	2.404, 2.391	641, 350
7	2.351	3, 13	2.357, 2.348	042, 142
11	2.327	28	2.327	632
8	2.279	8	2.279	342
5	2.242	4	2.244	123
6	2.231	3	2.234	12.0.0
2	2.186	2	2.184	323
4	2.172	1, 7	2.172, 2.170	841, 650
6	2.157	8	2.158	922
3	2.132	4	2.135	12.0.1
11	2.089	5, 20, 1	2.095, 2.087, 2.085	613, 033, 642
6	2.069	6	2.068	060
4	2.041	1	2.042	152
6	2.016	2, 1, 1	2.019, 2.017, 2.017	12.2.1, 11.3.1, 713
7	1.997	4	1.996	352
9	1.966	11	1.966	12.3.0
6	1.880	9, 4	1.880, 1.877	12.1.2, 660
12	1.849	19	1.848	942
8	1.814	2, 12	1.817, 1.813	661, 004
10	1.798	14, 1	1.796, 1.795	062, 10.0.3
4	1.770	4	1.769	15.1.0
6	1.728	11, 2	1.728, 1.728	12.3.2, 153
3	1.710	6	1.708	324
2	1.692	4	1.691	371
6	1.669	5, 12	1.671, 1.667	15.2.1, 662
3	1.661	5	1.660	12.5.0
2	1.643	2	1.641	12.0.3
2	1.621	3	1.619	12.5.1
5	1.590	10	1.590	15.1.2
6	1.553	2, 5, 5	1.556, 1.552, 1.551	634, 15.2.2, 080
6	1.515	15	1.514	15.4.1
4	1.491	2, 5, 1	1.495, 1.491, 1.490	15.3.2, 971, 14.1.3
3	1.452	3	1.450	934
3	1.427	1, 4, 3	1.428, 1.426, 1.424	16.3.2, 082, 15.4.2
4	1.409	1	1.410	125
6	1.371	2	1.371	615
5	1.334	1, 1	1.336, 1.333	464, 12.3.4
7	1.305	5, 1	1.304, 1.304	15.4.3, 664
6	1.298	2, 2	1.297, 1.296	915, 691
7	1.287	2, 1, 1	1.289, 1.286, 1.285	973, 982, 12.6.3

*For the calculated pattern, only reflections with intensities ≥ 1 are given; **for the unit-cell parameters calculated from single-crystal data; d_{calc} and I_{calc} were calculated using the STOE WinX^{Pow} software package (STOE WinX^{Pow}, 2002).

Single-crystal X-ray studies were carried out using an Xcalibur S CCD diffractometer. More than a hemisphere of three-dimensional data was collected. Crystal data, data collection information and structure refinement details are given in Table 3. Data reduction was performed using CrysAlisPro Version 1.171.35.21 (Agilent, 2012). The data were corrected for Lorentz and polarization effects. An empirical absorption correction using spherical harmonics, implemented in SCALE3 ABSPACK scaling algorithm, was applied. The structure was solved by direct methods and refined with the use of SHELX software package (Sheldrick, 2008) on the basis of 3516 independent reflections with $I > 2\sigma(I)$. A model for merohedral twinning with an inversion centre as a twinning operator was introduced with a twin ratio of 0.54:0.46. Atom coordinates and displacement parameters for the holotype flinteite are given in Table 4, selected interatomic distances in Table 5 and bond-valence calculations in Table 6.

Table 3. Crystal data, data collection information and structure refinement details for flinteite.

Formula weight*	302.09
Crystal system, space group, *Z*	Orthorhombic, $Pna2_1$, 12
Unit-cell dimensions	$a = 26.8090(10)$ Å
	$b = 12.4085(6)$ Å
	$c = 7.2512(3)$ Å
Volume	2412.19(18) Å^3
μ*	5.532 mm^{-1}
F(000)*	1729
Crystal size	0.06 × 0.12 × 0.18 mm
Data collection	XcaliburS CCD
Temperature	293(2) K
Radiation, wavelength	Mo$K\alpha$; $\lambda = 0.71073$ Å
θ range for data collection	3.04–28.28°
Reflections collected	19792
Unique reflections	5689 ($R_{int} = 0.0759$)
Unique reflections with $I > 2\sigma(I)$	3516
Structure solution	direct methods
Refinement method	full-matrix least-squares on F^2
Number of refined parameters	197
R_F/wR (F^2) ($I > 2\sigma(I)$)	0.0686/0.0898
GoF	1.051
$\Delta\rho_{max}/\Delta\rho_{min}$	0.756/-0.565 e/Å^3

* Calculated based on the e_{ref} values.

Table 4. Atom coordinates, equivalent displacement parameters (Å^2) and site occupancies for flinteite.

Site	*x*	*y*	*z*	U_{eq}	s.o.f.*
Zn(1)	0.07216(5)	0.42033(14)	0.75057(19)	0.0289(4)	Zn
Zn(2)	0.40545(5)	0.41780(13)	0.77926(17)	0.0296(5)	Zn
Zn(3)	0.74005(5)	0.41813(13)	0.74095(17)	0.0272(4)	Zn
K(1)	0.04391(8)	0.0836(2)	0.7831(5)	0.0613(10)	[27.2] $K_{0.87}Tl_{0.13}$
K(2)	0.37937(8)	0.0871(3)	0.7611(5)	0.0720(11)	[27.3] $K_{0.87}Tl_{0.13}$
K(3)	0.71030(9)	0.0849(3)	0.7290(5)	0.0562(11)	[24.0] $K_{0.92}Tl_{0.08}$
K(4)	0.33196(10)	0.6872(3)	0.7283(5)	0.0430(11)	[20.2] $K_{0.98}Tl_{0.02}$
K(5)	0.66580(10)	0.6859(3)	0.7425(6)	0.0476(11)	[20.1] $K_{0.98}Tl_{0.02}$
K(6)	0.99829(10)	0.6876(2)	0.7900(5)	0.0345(10)	[19.4] $K_{0.99}Tl_{0.01}$
Cl(1)	0.99149(10)	0.4416(3)	0.6815(6)	0.0406(9)	Cl
Cl(2)	0.11228(12)	0.5763(3)	0.8140(6)	0.0524(10)	Cl
Cl(3)	0.08633(15)	0.3058(4)	0.9838(6)	0.0632(13)	Cl
Cl(4)	0.11051(13)	0.3538(4)	0.4919(6)	0.0584(12)	Cl
Cl(5)	0.32343(11)	0.4351(3)	0.8088(7)	0.0699(14)	Cl
Cl(6)	0.44374(14)	0.5778(3)	0.8099(8)	0.0876(18)	Cl
Cl(7)	0.43542(15)	0.3131(4)	0.0016(6)	0.0887(19)	Cl
Cl(8)	0.43024(17)	0.3461(4)	0.5157(6)	0.0942(19)	Cl
Cl(9)	0.65905(11)	0.4356(3)	0.8026(7)	0.0681(14)	Cl
Cl(10)	0.77845(13)	0.5767(3)	0.6762(7)	0.0466(10)	Cl
Cl(11)	0.77610(13)	0.3606(3)	0.0083(5)	0.0451(9)	Cl
Cl(12)	0.75696(15)	0.2956(3)	0.5205(5)	0.0504(10)	Cl

*Site occupancies are based on e_{ref} values (given in square brackets).

Table 5. Selected interatomic distances (Å) for flinteite.

Zn(1) tetrahedron		K(3) polyhedron	
Zn(1) – Cl(1)	2.236(3)	K(3) – Cl(5)	3.098(4)
- Cl(3)	2.242(4)	- Cl(11)	3.231(5)
- Cl(2)	2.262(4)	- Cl(10)	3.259(6)
- Cl(4)	2.293(4)	- Cl(12)	3.269(5)
Zn(2) tetrahedron		- Cl(4)	3.270(5)
Zn(2) – Cl(8)	2.211(5)	- Cl(2)	3.360(5)
- Cl(5)	2.220(3)	K(4) polyhedron	
- Cl(7)	2.221(4)	K(4) – Cl(3)	3.179(5)
- Cl(6)	2.246(4)	- Cl(5)	3.191(5)
Zn(3) tetrahedron		- Cl(12)	3.197(5)
Zn(3) – Cl(9)	2.228(3)	- Cl(4)	3.211(5)
- Cl(12)	2.252(4)	- Cl(10)	3.284(5)
- Cl(10)	2.270(4)	- Cl(6)	3.342(5)
- Cl(11)	2.281(4)	- Cl(11)	3.360(5)
K(1) polyhedron		- Cl(9)	3.451(6)
K(1) – Cl(9)	3.099(4)	K(5) polyhedron	
- Cl(3)	3.318(6)	K(5) – Cl(9)	3.141(5)
- Cl(6)	3.355(4)	- Cl(11)	3.164(5)
- Cl(6)	3.449(7)	- Cl(12)	3.195(5)
- Cl(8)	3.466(6)	- Cl(7)	3.227(5)
- Cl(7)	3.552(5)	- Cl(8)	3.272(6)
- Cl(8)	3.716(5)	- Cl(2)	3.322(5)
- Cl(6)	3.834(7)	- Cl(10)	3.345(5)
- Cl(7)	3.968(7)	- Cl(5)	3.497(6)
K(2) polyhedron		K(6) polyhedron	
K(2) – Cl(1)	3.081(4)	K(6) – Cl(7)	3.155(5)
- Cl(2)	3.252(6)	- Cl(1)	3.158(5)
- Cl(4)	3.355(6)	- Cl(3)	3.175(5)
- Cl(11)	3.362(5)	- Cl(8)	3.196(5)
- Cl(10)	3.440(5)	- Cl(6)	3.261(5)
- Cl(7)	3.628(7)	- Cl(1)	3.272(5)
- Cl(8)	3.918(7)	- Cl(4)	3.304(5)
- Cl(12)	3.991(5)	- Cl(2)	3.358(4)
- Cl(2)	4.018(6)		
- Cl(3)	4.132(6)		

The crystal structure of flinteite (Fig. 4), as well as its synthetic end-member analogue (see below), consists of $ZnCl_4$ tetrahedra and K-centred polyhedra. Three crystallographically independent Zn sites centre isolated tetrahedra with average distances Zn(1)–Cl = Zn(3)–Cl = 2.258 and Zn(2)–Cl = 2.224 Å. Potassium cations are located in six crystallographically independent sites. The K(1) and K(2) cations centre nine- and ten-coordinate polyhedra, respectively, with six shorter K–Cl distances [3.099–3.552 Å for K(1) and 3.081–3.628 Å for K(2)]; other K–Cl bonds are elongated with three in the interval 3.716–3.968 Å for K(1) and four in the interval 3.918–4.132 Å for K(2). The K(3) cations occupy six-coordinate polyhedra with interatomic distances in the range 3.098–3.360 Å while K(4,5,6) centre eight-coordinate polyhedra with K–Cl distances varying from 3.179 to 3.451 Å [K(4)], from 3.141 to 3.497 Å [K(5)] and from 3.155 to 3.358 Å [K(6)]. The major part of Tl^+ admixture substituting K^+ is concentrated in the K(1,2,3) sites (Table 4).

Discussion

No halide minerals related to flinteite in terms of structure are known. The only earlier described natural halide with the formula A_2MX_4 (X = F, Cl, Br, I) is pseudocotunnite K_2PbCl_4. This mineral is insufficiently studied but obviously different, as well as synthetic K_2PbCl_4 (with the same unit-cell dimensions: orthorhombic, a = 11.80, b = 5.77, c = 9.82 Å; Campostrini *et al.*, 2011), from flinteite.

At the same time, flinteite is a natural analogue of a well-known synthetic room-temperature modification of K_2ZnCl_4 (space group $Pna2_1$, a = 26.66–27.25, b =

Table 6. Bond valence calculations for flinteite. Parameters are taken from Brese & O'Keeffe (1991).

	Zn(1)	Zn(2)	Zn(3)	K(1)	K(2)	K(3)	K(4)*	K(5)*	K(6)*	∑
Cl(1)	0.54				0.22				0.18	1.07
									0.13	
Cl(2)	0.51				0.14	0.11		0.11	0.10	0.99
					0.02					
Cl(3)	0.53			0.12	0.01		0.17		0.17	1.00
Cl(4)	0.46				0.10	0.13	0.15		0.12	0.96
Cl(5)		0.57				0.20	0.16	0.07		1.00
Cl(6)		0.53		0.10			0.11		0.13	0.97
				0.08						
				0.02						
Cl(7)		0.56		0.06	0.05			0.15	0.18	1.02
				0.02						
Cl(8)		0.58		0.08	0.02			0.13	0.16	1.01
				0.04						
Cl(9)			0.55	0.21			0.08	0.19		1.03
Cl(10)			0.49		0.08	0.13	0.13	0.11		0.94
Cl(11)			0.48		0.10	0.14	0.10	0.17		1.09
Cl(12)			0.52		0.02	0.13	0.16	0.16		0.99
∑	2.04	2.24	2.04	0.73	0.76	0.84	1.06	1.09	1.17	

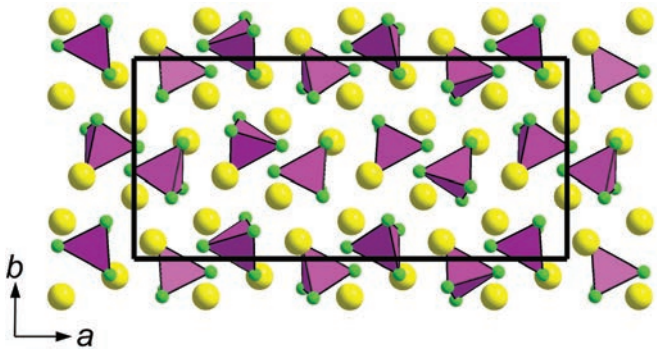

Fig. 4. The crystal structure of flinteite. $ZnCl_4$ tetrahedra are shown. K cations are large spheres. The unit cell is outlined. (online version in colour)

12.30–12.58, c = 7.21–7.26 Å; Mikhail & Peters, 1979; Quilichini *et al.*, 1988; Kusz & Kucharczyk, 1995; Kusz *et al.*, 1997; Ferrari *et al.*, 2001). This compound has been the focus of active investigations during the last 35 years because its room-temperature modification is considered as a prospective ferroelectric material. The high-temperature form of K_2ZnCl_4 is a typical representative of phases with one-dimensionally modulated incommensurate structures of the A_2BX_4 type. K_2ZnCl_4 undergoes a sequence of phase transitions characteristic for such crystals: a paraelectric phase (β-K_2SO_4 structure type, *Pnma*, a = 8.96, b = 7.30, c = 12.54 Å, Z = 4, $T > 553$ K) → an incommensurate phase ($403 < T < 553$ K) → a commensurable non-intrinsic ferroelectric phase ($Pna2_1$, Z = 12, $145 < T < 403$ K) (Kucharczyk *et al.*, 1982; Quilichini *et al.*, 1990; Kusz & Kucharczyk, 1995; Ferrari *et al.*, 2001). The latter is an analogue of the end-member flinteite. As reported in the above publications, this room-temperature modification of dipotassium tetrachlorzincate is stable at temperatures below 403 K (=130°C).

We believe that the flinteite studied by us at room temperature was formed as the result of a phase transition when cooling after the extraction of crystals of its proto-phase from hot cameras of fumaroles at the First scoria cone (the temperatures measured *in situ* during sampling were 180–290°C) and of the Arsenatnaya fumarole (300–360°C). We suppose that temperature of the phase transition from this hypothetical high-temperature modification (deposited directly from fumarolic gas as a volcanic sublimate) to flinteite is even lower than 403 K for its Tl- or Rb(Cs)-enriched varieties. Indeed, synthetic Tl_2ZnCl_4 demonstrates the above discussed phase transitions at 363 and 173 K, respectively (Shimizu *et al.*, 2005), and synthetic Rb_2ZnCl_4 at 302 and 189 K, respectively (Quilichini & Pannetier, 1983).

In the Glavnaya Tenoritovaya fumaroles, near-end-member flinteite (#6 in Table 1) was collected at 110°C and the temperature of formation of this assemblage including many highly hydrated minerals could not be significantly higher (Pekov *et al.*, 2015b). In this relatively low-temperature natural system, flinteite could crystallize directly, escaping a proto-phase step. Synthesis of its analogue under low-temperature conditions was reported, *e.g.*, from aqueous solution at 35°C (Takai *et al.*, 1995).

Flinteite, a common mineral in fumarolic deposits of the Northern field of the First scoria cone, is the major concentrator of thallium here. This rare element substitutes K (Tables 1 and 4) in the form of Tl^+ which, together with other mineralogical signs, indicates moderately oxidizing conditions in this mineral-forming system. In sublimates of these fumaroles we see minerals with S^{6+} (sulphur forms here only sulphates), both Se^{4+} and Se^{6+} (prevailing form of selenium is Se^{4+}: sofiite and zincomenite are common whereas olsacherite is rare), Fe^{3+} (hematite), both Mn^{2+}

(saltonseaite) and Mn^{4+} (hollandite) and Tl^{+} (flinteite). In other fumaroles of the First scoria cone another mineral of Tl^{+}, markhininite $TlBi(SO_4)_2$ was discovered as a primary, sublimate phase (Siidra *et al.*, 2014). In contrast, in fumaroles of the Second scoria cone, flinteite is almost Tl-free (##6–8 in Table 1) which is probably caused by a more strongly oxidizing character of volcanic gas here. In the Glavnaya Tenoritovaya fumarole, flinteite is associated with chrysothallite, $K_6Cu_6Tl^{3+}Cl_{17}(OH)_4 \cdot H_2O$, a mineral of trivalent thallium (Pekov *et al.*, 2015b). Thus, Tl admixture in flinteite could be considered as a geochemical indicator, the marker for oxidizing conditions in a fumarolic system.

In the Arsenatnaya fumarole, flinteite is significantly enriched in rubidium (up to 2.4 wt% Rb) and cesium (up to 2.2 wt% Cs): #8 in Table 1. Significant contents of Rb and Cs were earlier detected in some other minerals formed in fumaroles of the Second scoria cone. Their highest concentrations were reported for averievite $Cu_5O_2(VO_4)_2 \cdot n(Cs,K,Rb)Cl$ (0.5–1.1 wt% Rb_2O and 2.7–4.1 wt% Cs_2O; Starova *et al.*, 1997; Vergasova *et al.*, 1998) and parawulffite, ideally $K_5Na_3Cu_8O_4(SO_4)_8$ (1.2–1.7 wt% Rb_2O and 1.2–1.7 wt% Cs_2O; Pekov *et al.*, 2014b). Thus, flinteite from Arsenatnaya is the Rb-richest mineral known to date in fumaroles related to the Tolbachik volcano.

Acknowledgements: We thank two anonymous referees for valuable comments. This study was supported by the Russian Science Foundation, grant no. 14-17-00048. The technical support by the SPbSU X-Ray Diffraction Resource Center in the XRD powder-diffraction studies is acknowledged.

References

Agilent. (2012): CrysAlis PRO. Agilent Technologies, Yarnton, England.

Brese, N.E. & O'Keeffe, M. (1991): Bond-valence parameters for solids. *Acta Cryst.*, **B47**, 192–197.

Campostrini, I., Demartin, F., Gramaccioli, C.M., Russo, M. (2011): Vulcano: Tre Secoli di Mineralogia. Associazione Micro-mineralogica Italiana, Cremona.

Fedotov, S.A. & Markhinin, Y.K., eds. (1983): The Great Tolbachik Fissure Eruption. Cambridge University Press, New York, NY.

Ferrari, E.S., Roberts, K.J., Thomson, G.B., Gale, J.D., Catlow, C.R.A. (2001): Interatomic potential parameters for potassium tetrachlorozincate and their application to modelling its phase transformations. *Acta Cryst.*, **A57**, 264–271.

Kucharczyk, D., Paciorek, W., Kalicińska-Karut, J. (1982): X-ray study of the high-temperature phase transitions in K_2ZnCl_4. *Phase Trans.*, **2**, 277–283.

Kusz, J. & Kucharczyk, D. (1995): The comparative study of the commensurate structure of K_2ZnCl_4. *Appl. Crystallogr.*, **6**, 268–272.

Kusz, J., Pietraszko, A., Warczewski, J. (1997): X-ray study of the low temperature phase transitions in K_2ZnCl_4. *Phase Trans.*, **60**, 1–13.

Mikhail, I. & Peters, K. (1979): The structure of potassium tetrachlorozincate. *Acta Cryst.*, **B35**, 1200–1201.

Moyer, J.R., Evans, J.C., Lo, G.Y.-S. (1966): A Raman spectroscopic study of the molten salt system $ZnCl_2$–KCl. *J. Electrochem. Soc.*, **113**, 158–161.

Pekov, I.V., Zubkova, N.V., Yapaskurt, V.O., Belakovskiy, D.I., Lykova, I.S., Vigasina, M.F., Sidorov, E.G., Pushcharovsky, D.Yu. (2014a): New arsenate minerals from the Arsenatnaya fumarole, Tolbachik volcano, Kamchatka, Russia. I. Yurmarinite, $Na_7(Fe^{3+},Mg,Cu)_4(AsO_4)_6$. *Mineral. Mag.*, **78**, 905–917.

Pekov, I.V., Zubkova, N.V., Yapaskurt, V.O., Belakovskiy, D.I., Chukanov, N.V., Lykova, I.S., Savelyev, D.P., Sidorov, E.G., Pushcharovsky, D.Yu. (2014b): Wulffite, $K_3NaCu_4O_2(SO_4)_4$, and parawulffite, $K_5Na_3Cu_8O_4(SO_4)_8$, two new minerals from fumarole sublimates of the Tolbachik volcano, Kamchatka, Russia. *Can. Mineral.*, **52**, 699–716.

Pekov, I.V., Zubkova, N.V., Yapaskurt, V.O., Lykova, I.S., Belakovskiy, D.I., Vigasina, M.F., Sidorov, E.G., Britvin, S.N., Pushcharovsky, D.Yu. (2015a): New zinc and potassium chlorides from fumaroles of the Tolbachik volcano, Kamchatka, Russia: mineral data and crystal chemistry. I. Mellizinkalite, $K_3Zn_2Cl_7$. *Eur. J. Mineral.*, **27**, 247–253.

Pekov, I.V., Zubkova, N.V., Belakovskiy, D.I., Yapaskurt, V.O., Vigasina, M.F., Lykova, I.S., Sidorov, E.G., Pushcharovsky, D.Yu. (2015b): Chrysothallite $K_6Cu_6Tl^{3+}Cl_{17}(OH)_4 \cdot H_2O$, a new mineral species from the Tolbachik volcano, Kamchatka, Russia. *Mineral. Mag.*, **79**, in press.

Quilichini, M. & Pannetier, J. (1983): Neutron structural study of the successive phase transitions in Rb_2ZnCl_4. *Acta Cryst.*, **B39**, 657–663.

Quilichini, M., Heger, G., Schweiss, P. (1988): Neutron structural study of the ferroelectric phase of K_2ZnCl_4. *Ferroelectrics*, **79**, 117–120.

Quilichini, M., Bernede, P., Lefebvre, J., Schweiss, P. (1990): Neutron study of the normal-incommensurate phase transition in K_2ZnCl_4. *J. Phys. Condens. Matter*, **2**, 4543–4558.

Sheldrick, G.M. (2008): A short history of SHELX. *Acta Cryst.*, **A64**, 112–122.

Shimizu, F., Takashige, M., Yamaguchi, T., Kurihama, T., Suzuki, K. (2005): Possible existence of α–β phase transition in Tl_2ZnCl_4. *J. Korean Phys. Soc.*, **46**, 205–207.

Siidra, O.I., Vergasova, L.P., Krivovichev, S.V., Kretser, Y.L., Zaitsev, A.N., Filatov, S.K. (2014): Unique thallium mineralization in the fumaroles of Tolbachik volcano, Kamchatka peninsula, Russia. I. Markhininite, $Tl^{+}Bi(SO_4)_2$. *Mineral. Mag.*, **78**, 1687–1698.

Starova, G.L., Krivovichev, S.V., Fundamenskii, V.S., Filatov, S.K. (1997): The crystal structure of averievite, $Cu_5O_2(VO_4)_2 \cdot nMX$: comparison with related compounds. *Mineral. Mag.*, **61**, 441–446.

STOE $WinX^{Pow}$ Software (2002): STOE & CIE GmbH, Darmstadt, Germany.

Takai, S., Kawaji, H., Atake, T., Gesi, K. (1995): Phase transition and effect of small amount of water included in K_2ZnCl_4 crystal. *Netsu Sokutei*, **22**(1), 21–24.

Vergasova, L.P., Starova, G.L., Filatov, S.K., Ananiev, V.V. (1998): Averievite $Cu_5O_2(VO_4)_2 \cdot nMX$ – a new mineral of volcanic exhalations. *Doklady AN SSSR*, **359**, 804–807. (in Russian).

Received 31 January 2015
Modified version received 30 March 2015
Accepted 1 April 2015